

Engineering amine-modified ammonium polyphosphate for enhancing flame retardancy and smoke suppression of vinyl ester resin

Tao Chu^{a,c,1}, Yixia Lu^{d,1}, Boyou Hou^{a,c}, Zhezhe Zhou^a, Qingshan Yang^a, Yong Guo^a,
Pooya Jafari^a, Asim Mushtaq^a, Xuesen Zeng^a, Siqi Huo^{a,b,*}, Pingan Song^{a,c,*} 

^a Centre for Future Materials, University of Southern Queensland, Springfield 4300, Australia

^b School of Engineering, University of Southern Queensland, Springfield 4300, Australia

^c School of Agriculture and Environmental Science, University of Southern Queensland, Springfield 4300, Australia

^d College of Biological and Chemical Engineering, Jiaying University, Jiaying 314001, China

ARTICLE INFO

Keywords:

Vinyl ester resin
Ammonium polyphosphate
Surface modification
Flame retardancy
Smoke suppression

ABSTRACT

Vinyl ester resin (VER), as a common thermosetting resin, has been widely used in many engineering fields. However, VER suffers from intrinsic flammability, and it can't meet the increasingly stringent fire safety requirements. Ammonium polyphosphate (APP) is an environmentally friendly flame retardant, but it needs a high loading level when applied in VER. In this study, the trinity flame retardant (DO) was synthesized through cation exchange reactions between APP and ethylenediamine (EDA) and ethanalamine (EOA). The flame-retardant properties/mechanism and thermal stability of DO/VER composites were investigated in detail. Our results demonstrated that the modification of EDA and EOA allowed DO to achieve better carbonization ability and higher flame-retardant efficiency than APP. For instance, when the molar ratio of EDA and EOA was 3:1, the resultant 26 %DO₃₋₁/VER composite (DO₃₋₁ content: 26 wt%) achieved a limiting oxygen index (LOI) of 26.5 % and a vertical burning (UL-94) V-0 rating. Under the same flame retardant content, 26 % APP/VER composite only showed a LOI of 22.5 % and a UL-94 V-2 rating. Additionally, 26 %DO₃₋₁/VER exhibited 74.5 %, 61.5 % and 44.2 % decreases in peak heat release rate (PHRR), peak smoke production rate (PSPR) and total heat release (THR) in comparison to VER. Obviously, DO showed superior flame retardancy and smoke suppression due to the reinforcement effects of EDA and EOA on condensed/gas-phase flame retardancy. This work proposes a facile method for the creation of highly effective APP-based flame retardants by cation exchange, which can be applied to flame-retardant and smoke-suppressive VER.

1. Introduction

VER is a kind of widely applied thermosetting resin, which can be produced by the reaction of epoxy resin and acrylic acid or methacrylic acid [1–3]. VER features outstanding chemical stability and can be cured in a mild condition [4–6]. Usually, styrene is introduced into VER to act as a diluent and cross-linking agent due to its low viscosity [7–9]. Furthermore, due to the excellent chemical resistance and mechanical properties of VER, it has been widely used in storage tanks and pipelines, transportation, marine engineering, and construction fields [10–13]. Nonetheless, its inherent flammability limits its high-performance applications. Upon ignition, it burns violently and releases a great deal of toxic and black smoke [14–16]. Therefore, a lot of attempts have been

made to improve the flame retardancy and smoke suppression of VER. In the past, many researchers found that the halogenated VER exhibited high flame retardancy [17,18]. During combustion, VER releases halogen-containing radicals, which quench the high-energy ·H and ·OH radicals in the gas phase, terminating the combustion chain reaction [19,20]. However, halogen flame retardants are toxic and will cause long-term harm to human beings. For instance, the brominated ones will cause endocrine disruption and may have some adverse effects on human brain functions and neurodevelopment [21,22]. Therefore, most halogen flame retardants have been banned in many regions for the benefit of human beings and the environment.

The phosphorous-nitrogen (P-N) synergist flame retardants are reliable alternatives to halogen based flame retardants [23–25].

* Corresponding authors at: Centre for Future Materials, University of Southern Queensland, Springfield 4300, Australia.

E-mail addresses: sqhuo@hotmail.com, Siqi.Huo@unisoq.edu.au (S. Huo), pingansong@gmail.com, pingan.song@usq.edu.au (P. Song).

¹ T. Chu and Y. Lu equally contributed to this work and were listed as co-first authors.

Ammonium polyphosphate (APP), as a classic halogen-free and environmental-friendly P-N flame retardant, has been widely used in wood, unsaturated polyester resin (UPR), epoxy resin, and other polymers due to its high phosphorus/nitrogen content, and ability to form an intumescent protective char layer during combustion [26–30]. Although APP has multiple advantages, some drawbacks still exist, such as its poor compatibility with the polymer matrix and low flame-retardant efficiency. Thus, APP needs to combine with additional carbon sources and blowing agents to form an intumescent flame retardant (IFR) system to achieve high efficiency. The carbon sources and blowing agents also suffer from poor compatibility with the VER matrix, leading to unsatisfied comprehensive properties. Cation exchange is a common method to modify APP by using organo-amines [31,32]. Different organo-amines can endow APP with various performances. By simply blending them in ethanol/water solution, the organo-amine-modified APP can be obtained. Compared with other modification methods, such as microencapsulation, this technique is more cost-effective. Moreover, this method does not significantly change the APP's morphology and particle size, effectively avoiding particle aggregation. Therefore, the cation exchange method with organo-amines has become a mainstream strategy to enhance the performance of APP.

To reinforce the efficiency of APP in the VER system, several strategies have been explored. For instance, Zeng *et al.* reported the fabrication of the IFR-containing VER by using 1-oxo-4-hydroxymethyl-2,6,7-trioxo-1-phosphabicyclo[2.2.2]octane (PEPA) as a charring agent (10 wt%), APP as an acid source (10 wt%), and molybdenum trioxide (MoO_3) as a smoke suppressor (5 wt%). The resultant VER composite can achieve V-0 rating in the UL-94 test and an LOI of 31.0%. Furthermore, its PHRR and THR were decreased by 76% and 53%, respectively, compared with those of virgin VER [33]. Du *et al.* synthesized a microencapsulated APP (MAPP) using propargyl-terminated ethylene oxide-tetrahydrofuran copolyether and glycidyl azido polymer and applied it in VER. 10 wt% of MAPP enabled VER/MAPP composite to achieve an LOI value of 27.1% and 44% and 38% decreases in THR and total smoke production (TSP). However, the VER/MAPP composite cannot achieve a UL-94 V-0 rating even when the MAPP content was up to 20 wt% [34]. Although some progress had been obtained in the APP-containing VER systems, their flame retardant contents were still very high and cannot meet industrial requirements. Therefore, creating high-efficiency APP-based flame retardants is very necessary for developing flame-retardant, high-performance VER composites.

In this work, we developed high-efficiency trinity flame retardants (DO) through cation exchange reactions of APP with EDA and EOA, and three DO flame retardants with different molar ratios of EDA and EOA were obtained and applied in the fabrication of flame-retardant VER composites. In DO, the EDA and EOA parts can function as blowing agent and carbon source to strengthen the flame-retardant effect of APP. The influences of DO on fire retardancy, thermal properties, and smoke suppression were investigated by different tests, and the flame-retardant mechanism of DO was also studied comprehensively.

2. Experimental

2.1. Materials

Ammonium polyphosphate (APP) was purchased from Oxford technologies (Australia). Ethanolamine (EOA), ethylenediamine (EDA), and ethanol were purchased from Sigma-Aldrich (Australia). Vinyl ester resin (Hetron 922 PAW) was supplied by Allnex Resins (Australia).

2.2. Synthesis of DO

In a three-neck glass flask, 10 mL of EDA (0.15 mol) and 3 mL of EOA (0.05 mol) were dissolved in a mixed solution (400 mL of ethanol and 20 mL of water). Subsequently, 40 g of APP was added into the flask, and the resultant mixture was continuously stirred at 90 °C and 200 rpm for

4 h. After that, the crude product was obtained by filtration, and it was washed with ethanol until the filtrate became neutral. The product was then placed in a vacuum oven and dried at 60 °C for 12 h. The DO_{3-1} product (molar ratio of EDA and EOA = 3:1) with a yield of 95% was obtained. For DO_{1-1} and DO_{1-3} , the molar ratios of EDA to EOA were adjusted to 1:1 and 3:1, respectively.

2.3. Preparation of VER/DO composites

Flame retardants (20, 23 or 26 wt%), MEKP (1 wt%), and VER were mixed in a flask for 10 min at room temperature. The mixture was defoamed under vacuum for 3 min, and then poured into stainless steel moulds. It was cured at 70 °C for 3 h and 100 °C for 2 h. The resulting VER composites containing 20 wt% APP were named 20 %APP/VER, and the others were named 23 %APP/VER, 26 %APP/VER, 20 % DO_{1-1} /VER, 23 % DO_{1-1} /VER, 26 % DO_{1-1} /VER, 20 % DO_{1-3} /VER, 23 % DO_{1-3} /VER, 26 % DO_{1-3} /VER, 20 % DO_{3-1} /VER, 23 % DO_{3-1} /VER, and 26 % DO_{3-1} /VER, respectively.

2.4. Characterization

This section is given in [Supporting information](#).

3. Results and discussion

3.1. Characterization of DO

The synthesis route of DO is shown in Fig. 1a. This synthesis was based on a cation exchange reaction between ammonium polyphosphate and amine groups of EDA and EOA. To determine the successful preparation of DO, Fourier transform infrared spectroscopy (FTIR), X-ray photoelectron spectroscopy (XPS), scanning electron microscopy (SEM), and energy dispersive X-ray spectrometry (EDX) analyses were conducted to confirm the chemical structure of DO.

The FTIR spectra of DO_{1-1} , DO_{1-3} , DO_{3-1} , and APP are shown in Fig. 1b. The peaks located at 1430 cm^{-1} ($-\text{NH}_4^+$), 1256 cm^{-1} (P = O), 1010 cm^{-1} (PO_2), and 790 cm^{-1} (P-O-P) are derived from APP [35]. After the reaction with EDA and EOA, DO_{1-1} , DO_{1-3} , and DO_{3-1} exhibited characteristic peaks at 1634 and 1527 cm^{-1} , which were ascribed to the vibration of $-\text{NH}_3^+$ ion from ethylenediamine and ethanolamine, respectively [36,37]. This result indicated that both EDA and EOA parts were successfully grafted onto the surface of APP.

Fig. 1c and d displays the high-resolution XPS N_{1s} and C_{1s} spectra of APP and DO. The binding energy at 384.8, 286.7, and 288.8 eV correspond to C-H/C-C, C-O-C, and C-O bonds of APP, respectively [38,39]. A new peak appeared at 286.3 eV in the C_{1s} spectra of DO_{1-1} , DO_{1-3} , and DO_{3-1} , which was ascribed to the $-\text{C}-\text{NH}_2$ groups [40]. APP showed the characteristic peaks at 399.8 and 401.6 eV in its N_{1s} spectrum, belonging to the P-NH-P and $-\text{NH}_4^+$ groups, respectively [41]. DO only exhibited one N_{1s} peak at around 401.2 eV, which corresponds to the $-\text{NH}_4^+$ and $-\text{C}-\text{NH}_2$ group [37]. The N_{1s} peaks of DO_{3-1} , DO_{1-1} , and DO_{1-3} appeared 401.1, 401.3, and 401.5 eV, respectively. The different peak positions might be due to the different molar ratios of EDA to EOA in these flame retardants. The XPS results further confirmed the successful preparation of DO by the reaction between APP and EDA/EOA.

The surface morphology of APP and DO was investigated by SEM, with the images presented in Fig. 2. The pristine APP showed a smooth but cracked surface. In contrast, DO_{1-1} , DO_{1-3} , and DO_{3-1} presented fewer surface cracks, but their morphology and particle size were similar to those of APP. When the content of EDA was increased, the DO surface became smoother and even agglomerated, which was probably because EDA served as a crosslinking agent. The EDX mappings of APP and DO are presented in Fig. S1. The EDX mappings confirmed the uniform distribution of C, N, O and P elements on the DO surface.

The thermogravimetric (TG) and derivative thermogravimetric (DTG) curves of DO and APP under a nitrogen atmosphere are presented

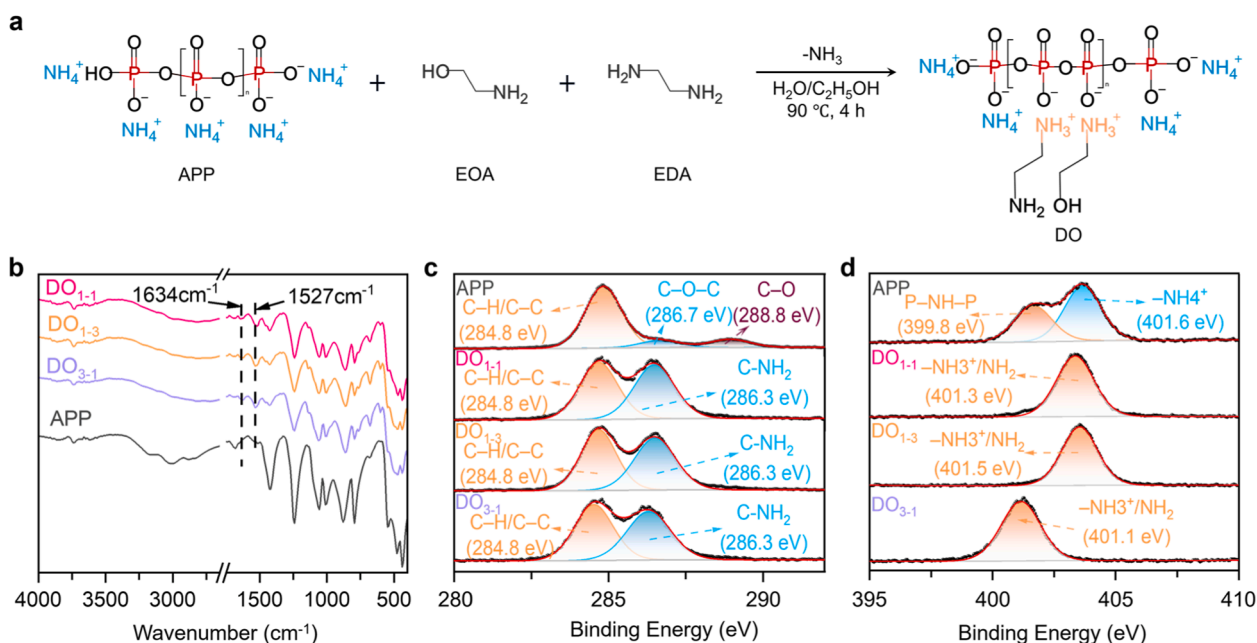


Fig. 1. (a) Synthesis route of DO, (b) FTIR spectra of DO₃₋₁, DO₁₋₁, DO₁₋₃, and APP, and (c, d) C_{1s} and N_{1s} spectra of APP and DO.

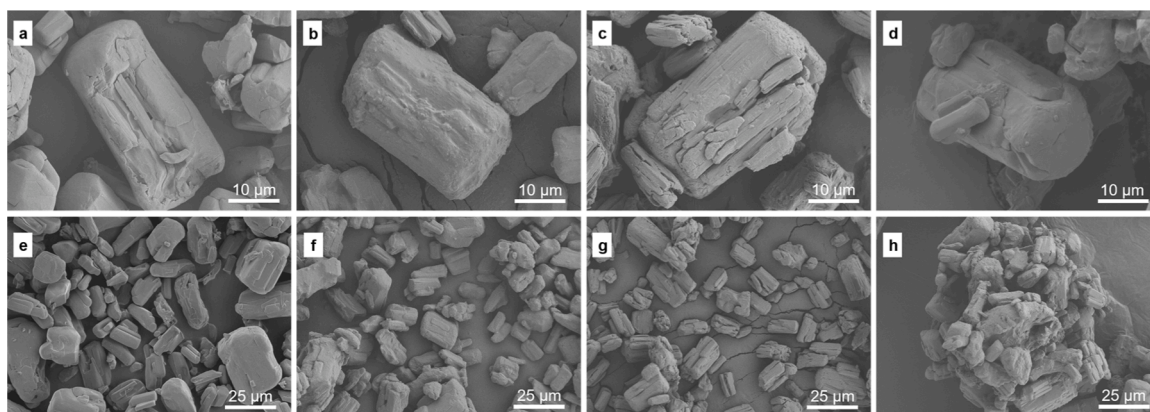


Fig. 2. SEM images of (a, e) APP, (b, f) DO₁₋₁, (c, g) DO₁₋₃, and (d, h) DO₃₋₁ under different magnifications.

in Fig. 3a and b. The initial degradation temperature (temperature at 5 % mass loss, T_i) of DO₃₋₁, DO₁₋₁, DO₁₋₃, and APP was 220, 223, 303, and 309 °C, respectively. The introduction of EDA and EOA reduced the T_i of DO, and the increase in the amount of EOA led to the increased T_i . This was probably caused by the earlier degradation of EDA and EOA parts compared with pristine APP. Similar to the T_i , the temperature at maximum mass loss rate (T_{max}) was also increased with the increasing content of EOA salt. All these results confirmed that DO was fabricated by the reaction between APP and EDA/EOA.

3.2. Thermal properties of VER and its composites

The TG and DTG curves of VER and its composites under in and air conditions are displayed in Fig. 3. The T_i , T_{max} , maximum weight loss rate (R_{max}) and residue (at 800 °C) are listed in Table 1. In nitrogen condition, the T_i and T_{max} of virgin VER were 334 and 400 °C, respectively, and it exhibited a single degradation stage, caused by the scission of the cross-linked network (Fig. 3b and e). The residue of VER was only 1.7 wt%. With the introduction of APP and DO, the T_i values of VER composites were decreased. In addition, new peaks emerged between 339 and 349 °C in the DTG curves of the APP- and DO-containing VER composites, demonstrating that their decomposition became two stages.

These new peaks were ascribed to the early degradation of APP and DO. Then, the degraded flame retardants began to release pyrophosphoric acid and metaphosphoric acid under heating [42]. These P-containing products dehydrated and reacted with the VER matrix to form a cross-linked char layer, which brought about reduced R_{max} and increased residue (Table 1). For instance, the residue of 26 % DO₃₋₁/VER at 800 °C reached 21.0 wt%, which was increased by 11.3 folds relative to that of VER.

Under air atmosphere, all APP and DO containing VER composites showed additional degradation stages after the main network decomposition, which was related to the thermal-oxidation decomposition of the formed char residues (Fig. 3c and f). The final T_{max} values of 26 % APP/VER, 26 % DO₁₋₁/VER, 26 % DO₁₋₃/VER, and 26 % DO₃₋₁/VER were 670, 702, 674, and 717 °C, respectively. All DO-containing VER composites showed higher T_{max} than the APP-containing VER composite, demonstrating that the char layers formed from DO-containing VER composites were more stable. For the DO-containing VER composites, their residues followed the trend: 26 % DO₁₋₃/VER > 26 % DO₁₋₁/VER > 26 % DO₃₋₁/VER. This demonstrated the positive effect of EDA parts in DO on promoting the carbonization of the VER matrix. Thus, all DO flame retardants can promote the carbonization of VER in elevated temperatures, among which DO₃₋₁ has the best promotion effect. The

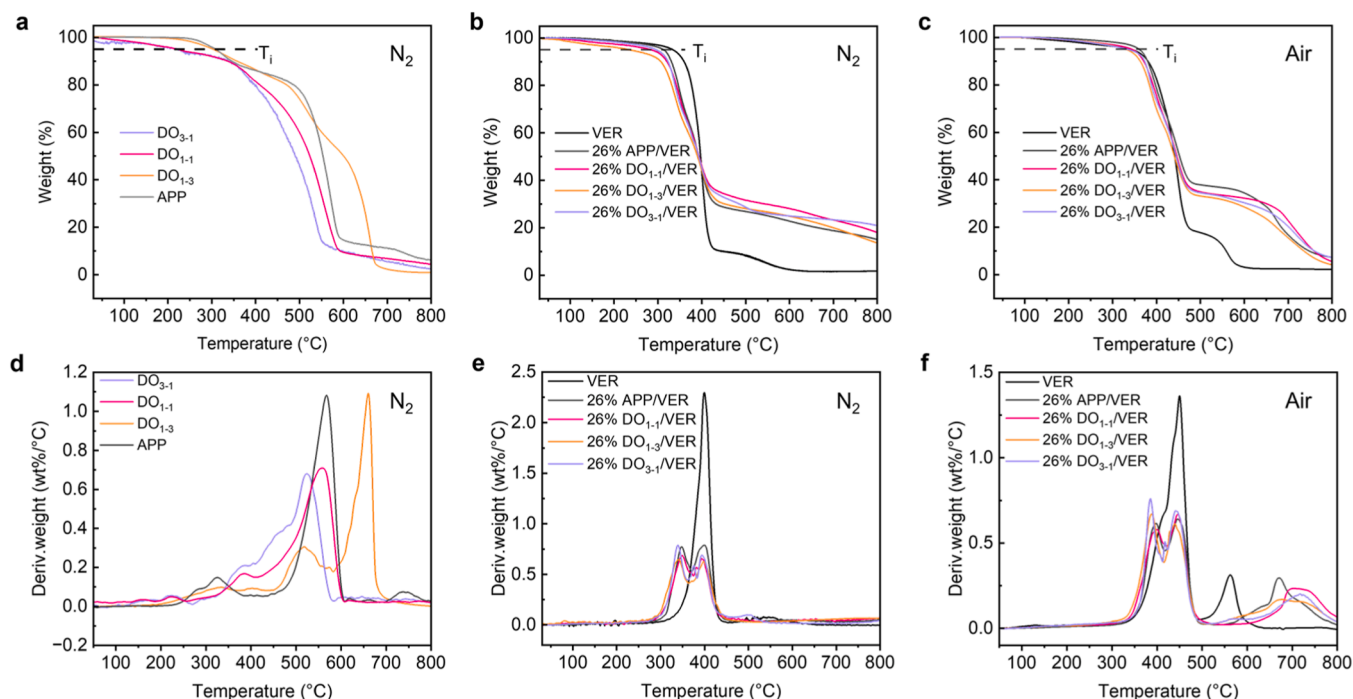


Fig. 3. (a, d) TG and DTG curves of DO₃₋₁, DO₁₋₁, DO₁₋₃, and APP under N₂ atmosphere; (b, e) TG and DTG curves of VER and its composites under N₂ atmosphere; and (c, f) TG and DTG curves of VER and its composites under air atmosphere.

Table 1

Thermal stability data of VER and its composites under nitrogen and air atmosphere.

Sample	26 % VER	26 % APP/VER	26 % DO ₁₋₁ /VER	26 % DO ₁₋₃ /VER	26 % DO ₃₋₁ /VER
T_i^a (°C)	334	313	283	236	296
T_{max}^a (°C)	400	348/400	349/393	340/397	339/393
R_{max}^a (wt %/°C)	2.3	0.8/0.8	0.7/0.7	0.6/0.6	0.8/0.7
Residue ^a (wt %)	1.7	15.1	18.2	13.6	21.0
T_i^b (°C)	338	360	343	329	327
T_{max}^b (°C)	449/562	397/447/670	399/446/702	387/439/674	384/440/717
R_{max}^b (wt %/°C)	1.4/0.3	0.6/0.6/0.3	0.6/0.6/0.2	0.7/0.6/0.2	0.8/0.7/0.2
Residue ^b (wt%)	2.2	7.4	5.7	4.3	7.4

^a Under nitrogen atmosphere

^b Under air atmosphere

introduction of DO also brought about the increased glass transition temperature (T_g) of VER (Table S1), which was probably because the -NH₂ groups on the DO surface participated in the curing process of VER, resulting in the increased crosslinking density.

3.3. Flame retardancy of VER and its composites

LOI and UL-94 tests have been widely used to evaluate the self-extinguish ability and flame retardancy of different materials. Therefore, the flame retardancy of VER and its composites were examined by LOI and UL-94 tests, with the related data listed in Table S1. As illustrated in Table S1, the LOI value of pure VER was only 16.0 %, indicating that it can be easily ignited in air atmosphere and burned violently. Also, during the UL-94 test, once VER sample was ignited, it cannot self-extinguish and released a great deal of black smoke, without any residue left (Fig. 4a). Hence, it cannot achieve any UL-94 rating. When APP was introduced, the LOI value of the APP-containing VER

composite can be up to 22.5 %, and the increasing APP content led to the weakening of flame and less smoke production during combustion. During the UL-94 test, the 26 %APP/VER composite extinguished within 1 s after the first ignition and within 15 s after the second ignition, thus it passed the UL-94 V-1 classification (Fig. 4a and Table S1). When replacing APP with DO, better flame retardancy (higher LOI value and UL-94 rating) can be achieved. For instance, the LOI values of 26 % DO₁₋₁/VER, 26 %DO₁₋₃/VER and 26 %DO₃₋₁/VER were increased to 25.0 %, 23.5 % and 26.5 %, respectively. Moreover, both 26 %DO₁₋₁/VER and 26 %DO₃₋₁/VER samples showed a UL-94 V-0 rating, demonstrating superior self-extinguishing performances (Fig. 4a and Table S1). The better flame retardancy of 26 %DO₁₋₁/VER and 26 %DO₃₋₁/VER than 26 %DO₁₋₃/VER was mainly due to the promotion effect of EDA parts on the carbonization of the VER matrix during combustion.

The cone calorimetry test (CCT) is an effective way to measure the heat release and smoke production of various materials in a real-fire situation [6,43]. Thus, the CCTs of VER, 26 %APP/VER, 26 % DO₁₋₁/VER, 26 %DO₁₋₃/VER, and 26 %DO₃₋₁/VER were conducted. The heat release rate (HRR), total heat release (THR), smoke production rate (SPR), and total smoke produced (TSP) curves are displayed in Fig. 4b-e. The related CCT data are listed in Table 2, including the time to ignition (TTI), PHRR, THR, peak smoke production rate (PSPR), TSP, carbon monoxide yield (YCO), carbon dioxide yield (YCO₂), and char residue after test. The virgin VER displayed the lowest TTI (17 s) and the highest PHRR (1062 kW/m²) and THR (86 MJ/m²) among all samples, demonstrating high flammability. After incorporating APP and DO, the resultant VER composites showed improved flame retardancy. The TTI values of all APP- and DO-containing VER composites were increased, demonstrating that people had more time to escape in a fire. 26 % DO₃₋₁/VER had the highest TTI of 50 s, indicative of superior anti-ignition ability. The VER composites exhibited significantly reduced PHRR values. Compared with VER, the PHRR values of 26 % APP/VER, 26 %DO₁₋₁/VER, 26 %DO₁₋₃/VER, and 26 %DO₃₋₁/VER were decreased by 70.0 %, 76.9 %, 76.6 %, and 74.5 %, respectively. In addition, all VER composites showed lower THR than VER. The THR values of 26 %APP/VER, 26 %DO₁₋₁/VER, 26 %DO₁₋₃/VER, and 26 % DO₃₋₁/VER were 38.4 %, 25.6 %, 16.3 %, and 44.2 % lower than that of

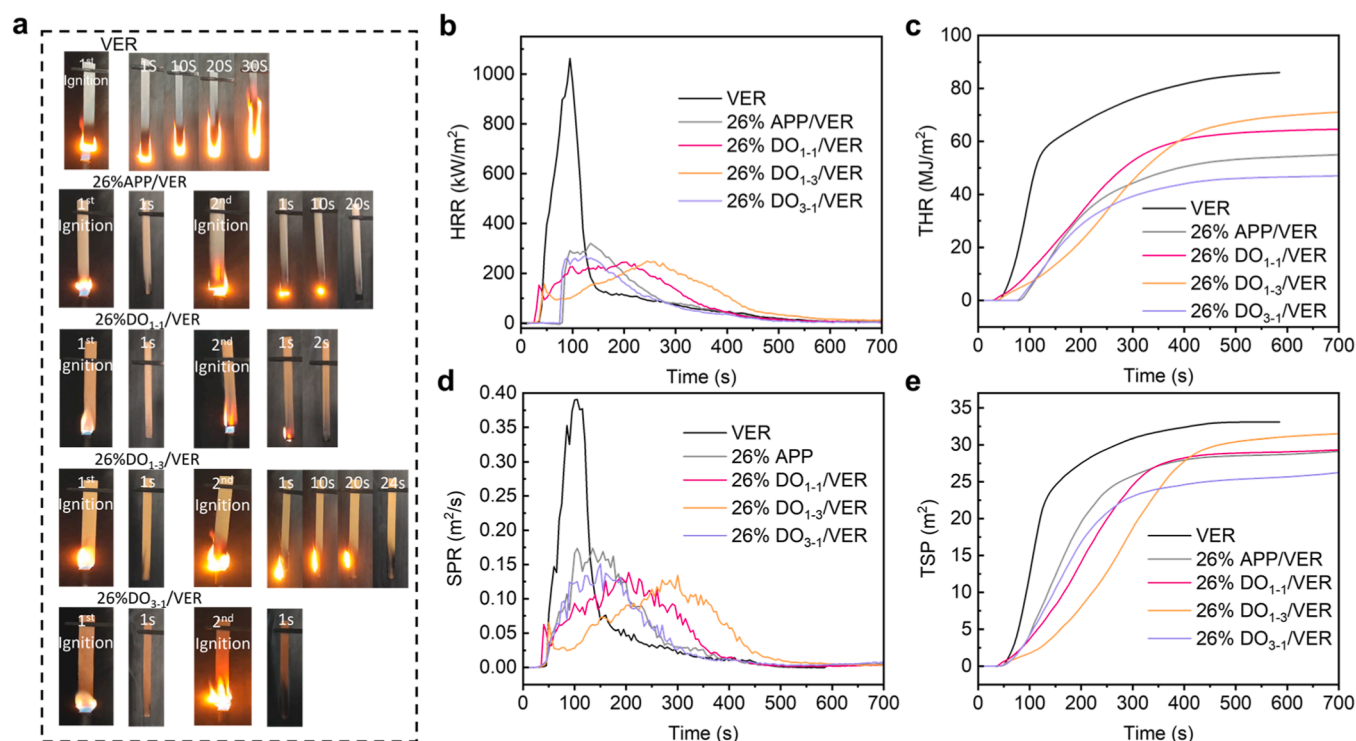


Fig. 4. (a) Digital photos of the burning behaviors for VER and its composites in the UL-94 tests, and (b) HRR, (c) THR, (d) smoke production rate (SPR), and (e) TSP curves of VER and its composites.

Table 2

The CCT data of VER and its composites.

Sample	TTI (s)	PHRR (kW/m ²)	THR (MJ/m ²)	PSPR (m ² /s)	YCO (g/s)	TSP (m ²)	YCO ₂ (g/s)	Char ^a (%)	FPI (m ² s/kW)	FGI (kW/m ² /s)
VER	17	1062	86	0.39	0.1	33	7.2	0.1	0.016	11.1
26 %APP/VER	38	319	53	0.17	0.1	31	4.6	28.0	0.119	2.37
26 %DO ₁₋₁ /VER	41	245	64	0.13	0.1	29	4.2	29.0	0.167	1.20
26 %DO ₁₋₃ /VER	41	249	72	0.13	0.09	29	3.6	30.5	0.164	1.01
26 %DO ₃₋₁ /VER	50	271	48	0.15	0.08	26	4.2	25.0	0.185	2.17

^a Char: Char residue after CCT.

VER. For 26 %DO₁₋₃/VER, and 26 %DO₁₋₁/VER, they were easier to ignite than 26 %DO₃₋₁/VER, as reflected by their lower TTI. This was probably because the abundant hydroxyl groups in DO₁₋₃ and DO₁₋₁ promoted the thermal degradation of APP during combustion [44]. The phosphorus-containing decomposition products of DO₁₋₃ and DO₁₋₁ facilitated the rapid formation of protective char layers. However, these chars were not stable and strong enough, leading to the broad peaks at 100–400 s in the HRR curves of 26 %DO₁₋₁/VER and 26 %DO₁₋₃/VER and their higher THR [45]. This analysis was further confirmed by the defective char residues of 26 %DO₁₋₁/VER and 26 %DO₁₋₃/VER after CCTs in Fig. S2. The 26 %APP/VER char also showed a discontinuous surface, demonstrating the unsatisfied carbonization-promoting effect of APP. In contrast, the 26 %DO₃₋₁/VER char had a dense surface with a high expansion height (17 mm), thus effectively suppressing heat release.

The smoke suppression ability of APP and DO in the VER matrix was also compared. As illustrated in Fig. 4d and Table 2, the introduction of APP and DO significantly reduced the PSPR of VER composites, and the DO-containing VER samples showed lower PSPR values than the APP-containing VER sample. Compared with VER, the PSPR values of 26 %DO₁₋₁/VER, 26 %DO₁₋₃/VER, and 26 %DO₃₋₁/VER were reduced by 66.7 %, 66.7 %, and 61.5 %, respectively. Meanwhile, the TSP values of the DO-containing VER samples were all lower than that of the APP-containing VER sample. All these results confirmed the enhanced

smoke suppression effect of DO due to the incorporation of EDA and EOA. The enhanced smoke suppression performances of the DO-containing VER composites can also be confirmed by their reduced YCO₂. Obviously, the introduction of EDA and EOA reinforced the carbonization-promoting effect of APP, which led to enhanced flame retardancy and smoke suppression of 26 %DO₁₋₁/VER, 26 %DO₁₋₃/VER, and 26 %DO₃₋₁/VER [46]. The fire performance index (FPI) and the fire growth index (FGI) are two key parameters used to assess the fire hazard of materials. The higher the FPI, the less flammable the material is, and the lower the FGI, the slower the fire spreads. As shown in Table 2, pure VER exhibited the lowest FPI of 0.016 m²s/kW and the highest FGI of 11.1 kW/m²/s, showing high fire hazard. After incorporating the flame retardants, the FPI was increased and the FGI was reduced, indicating enhanced fire resistance and reduced flame propagation. 26 %DO₃₋₁/VER showed the highest FPI value of 0.185 m²s/kW and 26 %DO₁₋₃/VER presented the lowest FGI value of 1.01 kW/m²/s. All DO/VER composites showed higher FPI and lower FGI than APP/VER, indicating that DO featured higher flame-retardant efficiency than APP.

The SEM images and Raman spectra of the residual chars for VER and its composites after CCTs are presented in Fig. 5. Obviously, 26 %APP/VER, 26 %DO₁₋₁/VER, and 26 %DO₁₋₃/VER generated crack char layers with abundant pores on their surface after CCTs (Fig. 5a). By contrast, the 26 %DO₃₋₁/VER char was more continuous and compact, with

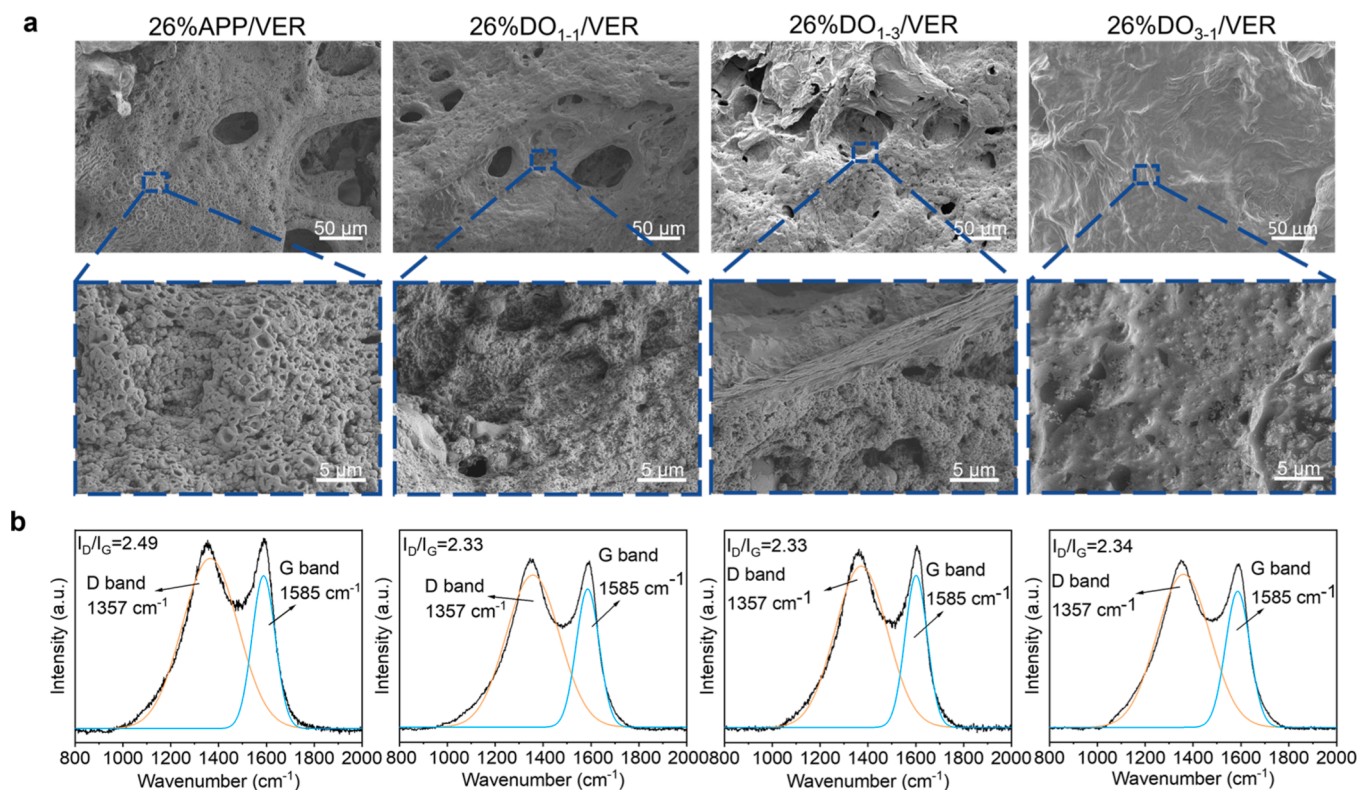


Fig. 5. (a) SEM images and (b) Raman spectra of residual chars after CCTs.

nearly no holes existed, and thus it can suppress the heat release and smoke generation more effectively during combustion. All Raman spectra in Fig. 5b show the D band and G band at 1357 and 1585 cm^{-1} , which belong to amorphous carbon atoms to graphitized carbon atoms, respectively [47,48]. The smaller the integrated area ratio of D band to G band (I_D/I_G), the higher graphitization degree and better protective effect [49,50]. The 26 %DO₁₋₁/VER, 26 %DO₁₋₃/VER, and 26 %DO₃₋₁/VER chars illustrated lower I_D/I_G values than 26 %APP/VER char, indicative of their higher graphitization degree due to the introduction of EDA and EOA [51]. Therefore, the introduction of EDA and EOA into APP helped to improve its flame-retardant and smoke-suppressive performances by enhancing the carbonization-promoting effect.

3.4. Flame retardant mechanism

The thermogravimetric-infrared spectroscopy (TG-IR) tests were performed on VER, 26 %APP/VER, and 26 %DO₃₋₁/VER to study their pyrolysis behaviors under heating, with the results listed in Fig. 6. As shown in Fig. 6a and a₁, the decomposition volatile of VER included aromatic (700 cm^{-1}), anhydride (1764 cm^{-1}), ester (1265 cm^{-1}), and hydrocarbons (3070 cm^{-1}) [52–54]. 26% APP/VER and 26 %DO₃₋₁/VER composites displayed similar gaseous products to VER under heating (Fig. 6b and c), but the absorption intensity was significantly reduced, demonstrating that less gaseous products were released. In addition, after introducing APP and DO, some new products emerged at 3746 cm^{-1} (H_2O), 3650 cm^{-1} (P-OH), and 960 – 930 cm^{-1} (NH_3) (Fig. 6b₁ and c₁) [55,56]. These new products were related to the decomposition of DO and APP, and the released H_2O and NH_3 contributed to diluting the concentration of flammable gases. Meanwhile, the P-OH-containing fragments can be further degraded into phosphorus-based radicals to terminate the combustion reaction. Notably, compared with 26 %APP/VER, 26 %DO₃₋₁/VER released less ester/aromatic-containing products and CO_2 under heating (Fig. 6d and f), which was conducive to suppressing combustion.

According to the above analyses, the flame-retardant mechanism of DO can be proposed as follows. In the first stage, DO started to dehydrate, releasing H_2O gas and forming the P-N-C-derived precursors. As the temperature increased, the precursors undertook two decomposition pathways. The first pathway was to release NH_3 by the scission of the P-N bond, forming metaphosphoric acid, phosphorus-derived radicals, alkane, and amine-derived radicals. Another degradation pathway was the further dehydration of the precursors. Subsequently, the formed viscous char layers covered the matrix surface, which contained P-O-P, P-O-C, and aromatic structures. Finally, abundant NH_2 , H_2O and other gases were released during combustion, leading to the formation of intumescent char layer. The possible charring process of DO during combustion is shown in Scheme 1.

4. Conclusions

In this work, the EDA/EOA-modified APP (DO) was successfully synthesized by a simple cation-exchange method. The resultant DO/VER composites exhibited lower R_{max} and higher residues at high temperatures, demonstrating enhanced carbonization ability. Notably, DO/VER composites showed better flame retardancy than VER and APP/VER composites, and 26 %DO₃₋₁/VER showed the highest LOI of 26.5 %, with a UL-94 V-0 rating. Moreover, 26 %DO₃₋₁/VER showed 74.5 %, 61.5 % and 44.2 % reductions in PHRR, PSPR and THR relative to VER, and its TTI was prolonged to 50 s, demonstrating obviously enhanced flame retardancy and smoke suppression. Clearly, introducing EDA and EOA can enhance the carbonization-promoting effect of APP and also strengthen its gas-phase flame-retardant effect. Hence, this work provides a facile strategy to prepare high-efficiency APP flame retardants for addressing the flammability issue of VER.

CRedit authorship contribution statement

Hou Boyou: Writing – review & editing. **Zhou Zhezhe:** Writing – review & editing. **Chu Tao:** Writing – original draft, Methodology,

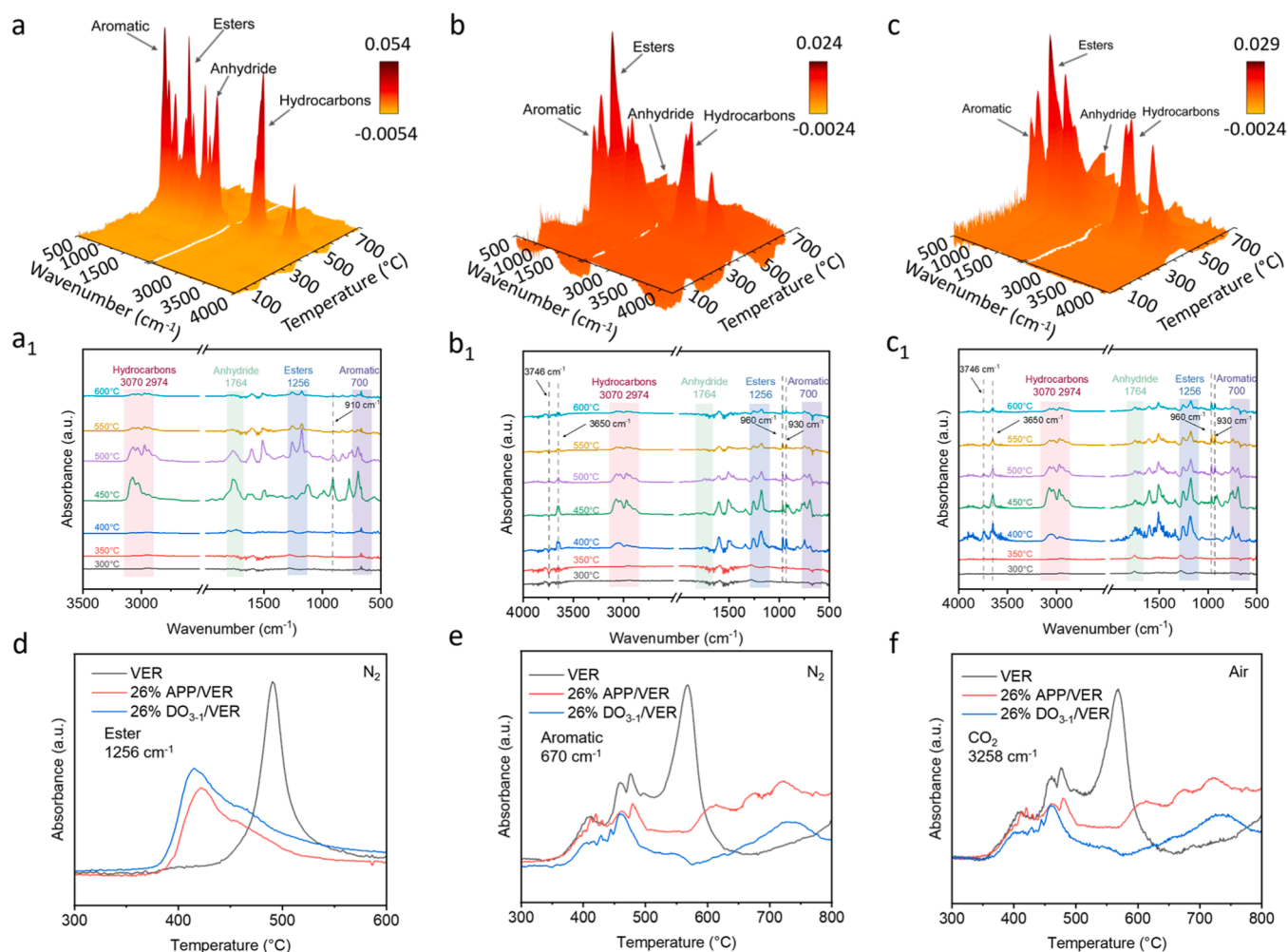
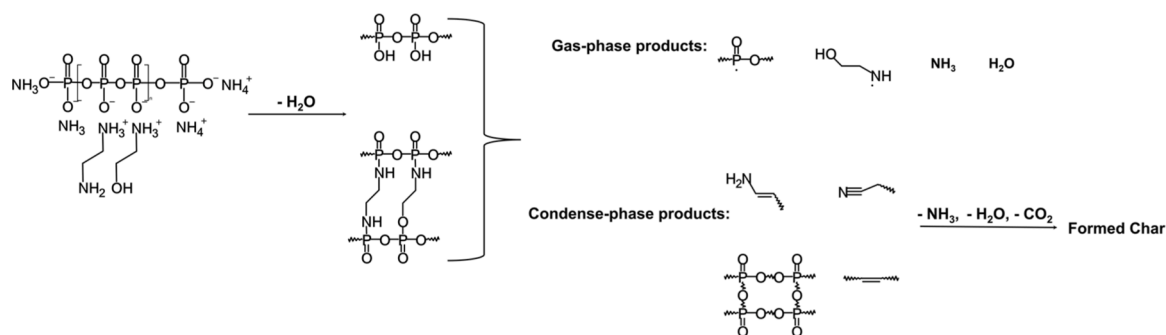


Fig. 6. (a-c) 3D TG-IR spectra of gaseous products for VER, 26 %APP/VER, and 26 %DO₃₋₁/VER, (a₁-c₁) FTIR spectra of gaseous products for VER, 26 %APP/VER, and 26 %DO₃₋₁/VER at different temperatures, and (d-f) absorbance vs. temperature curves of VER, 26 %APP/VER, and 26 %DO₃₋₁/VER at the wavenumbers of 1256, 670, and 3258 cm⁻¹.



Scheme 1. Illustration of possible charring process of DO during combustion.

Investigation, Data curation. **Lu Yixia:** Data curation. **Jafari Pooya:** Methodology. **Mushtaq Asim:** Methodology. **Yang Qingshan:** Writing – review & editing. **Guo Yong:** Writing – review & editing. **Zeng Xuesen:** Writing – review & editing. **Huo Siqi:** Writing – review & editing. **Song Pingan:** Writing – review & editing, Conceptualization.

Declaration of Competing Interest

The authors declare that they have no known competing financial interests or personal relationships that could have appeared to influence

the work reported in this paper.

Acknowledgments

This work was funded by the Australian Research Council (Nos. LP230100278, DP240102628, and DE230100616).

Appendix A. Supporting information

Supplementary data associated with this article can be found in the

online version at doi:10.1016/j.conbuildmat.2025.141174.

Data Availability

No data was used for the research described in the article.

References

- [1] S. Jaswal, B. Gaur, New trends in vinyl ester resins, *Rev. Chem. Eng.* 30 (2014) 567–581.
- [2] A. Joseph, Introduction to Vinyl Ester Resin. Synthesis, Curing Behaviour and Its Properties, Vinyl Ester-Based Biocomposites, CRC Press, 2023, pp. 1–24.
- [3] X. Zhang, W. Zhang, W. Zhang, R. Yang, Enhanced mechanical and flame retardancy properties of vinyl ester resin systems with the synthesis of two flame retardants with vinyl group, *Polym. Int.* 69 (12) (2020) 1196–1206.
- [4] İ. Kartal, G. Nayci, H. Demirer, The effect of chestnut wood flour size on the mechanical properties of vinyl ester composites, *Emerg. Mater. Res.* 9 (3) (2020) 960–965.
- [5] S.M. Seraji, P. Song, R.J. Varley, S. Bourbigot, D. Voice, H. Wang, Fire-retardant unsaturated polyester thermostets: the state-of-the-art, challenges and opportunities, *Chem. Eng. J.* 430 (2022) 132785.
- [6] J. Zhang, Y. Fang, A. Zhang, Y. Yu, L. Liu, S. Huo, X. Zeng, H. Peng, P. Song, A Schiff base-coated ammonia polyphosphate for improving thermal and fire-retardant properties of unsaturated polyester, *Prog. Org. Coat.* 185 (2023) 107910.
- [7] A.R. Jagtap, A. More, Developments in reactive diluents: a review, *Polym. Bull.* 79 (8) (2022) 5667–5708.
- [8] J. Thomason, G. Xypolias, Investigation of the effects of scale and cure environment on the properties of vinyl ester polymer, *Polym* 307 (2024) 127344.
- [9] Y.Z. Zhao, Y. Chu, Y.J. Xu, P. Zhu, Y.Z. Wang, Highly flame-retardant vinyl ester resins with well-balanced comprehensive performance, *Chem. Eng. J.* 464 (2023) 142659.
- [10] F. Rubino, A. Nisticò, F. Tucci, P. Carbone, Marine application of fiber reinforced composites: a review, *J. Mar. Sci. Eng.* 8 (1) (2020) 26.
- [11] S.O. Okuma, M. Obaseki, D.O. Ofuyekpone, O.E. Ashibudike, A review assessment of fiber-reinforced polymers for maritime applications, *J. Adv. Ind. Technol. Appl.* 4 (1) (2023) 17–28.
- [12] F.G. Alabtah, E. Mahdi, F.F. Eliyan, The use of fiber reinforced polymeric composites in pipelines: a review, *Compos. Struct.* 276 (2021) 114595.
- [13] H.Z. Farahani, A. Farahani, P. Fakharian, D. Jahed Armaghani, Experimental study on mechanical properties and durability of polymer silica fume concrete with vinyl ester resin, *Materials* 16 (2) (2023) 757.
- [14] X. Zhang, W. Zhang, Y.T. Pan, L. Qian, Z. Qin, W. Zhang, Synthesis and performance of intrinsically flame-retardant, low-smoke biobased vinyl ester resin, *React. Funct. Polym.* 171 (2022) 105158.
- [15] X. Zhang, W. Zhang, G. Zeng, J. Du, W. Zhang, R. Yang, The effect of different smoke suppressants with APP for enhancing the flame retardancy and smoke suppression on vinyl ester resin, *Polym. Eng. Sci.* 60 (2) (2020) 314–322.
- [16] S. Ji, H. Duan, Y. Chen, D. Guo, H. Ma, A novel phosphorus/nitrogen-containing liquid acrylate monomer endowing vinyl ester resin with excellent flame retardancy and smoke suppression, *Polym* 207 (2020) 122917.
- [17] E. Can, J. La Scala, J. Sands, G. Palmese, The synthesis of 9–10 dibromo stearic acid glycidyl methacrylate and its use in vinyl ester resins, *J. Appl. Polym. Sci.* 106 (6) (2007) 3833–3842.
- [18] G. Chigwada, P. Jash, D.D. Jiang, C.A. Wilkie, Fire retardancy of vinyl ester nanocomposites: synergy with phosphorus-based fire retardants, *Polym. Degrad. Stab.* 89 (1) (2005) 85–100.
- [19] S. Dev, P.N. Shah, Y. Zhang, D. Ryan, C.J. Hansen, Y. Lee, Synthesis and mechanical properties of flame retardant vinyl ester resin for structural composites, *Polymers* 133 (2017) 20–29.
- [20] M. Lewin, E.D. Weil, Mechanisms and modes of action in flame retardancy of polymers, *Fire Retard. Mater.* 1 (2001) 31–68.
- [21] J.L. Lyche, C. Rosseland, G. Berge, A. Polder, Human health risk associated with brominated flame-retardants (BFRs), *Environ. Int.* 74 (2015) 170–180.
- [22] Z. Ma, J. Feng, S. Huo, Z. Sun, S. Bourbigot, H. Wang, J. Gao, L.C. Tang, W. Zheng, P. Song, Mussel-inspired, self-healing, highly effective fully polymeric fire-retardant coatings enabled by group synergy, *Adv. Mater.* 36 (44) (2024) 2410453.
- [23] Y. Xue, M. Zhang, S. Huo, Z. Ma, M. Lynch, B.T. Tuten, Z. Sun, W. Zheng, Y. Zhou, P. Song, Engineered functional segments enabled mechanically robust, intrinsically fire-retardant, switchable, degradable polyurethane adhesives, *Adv. Funct. Mater.* 34 (49) (2024) 2409139.
- [24] Y. Lu, J. Feng, T. Chu, S. Huo, H. Xie, Z. Xu, H. Wang, P. Song, A 2D biobased P/N-containing aggregate for boosting fire retardancy of PA6/aluminum diethylphosphinate via synergy, *J. Mater. Sci. Technol.* 198 (2024) 73–82.
- [25] G. Ye, C. Wang, Q. Zhang, P. Song, H. Wang, S. Huo, Z. Liu, Bio-derived Schiff base vitrimer with outstanding flame retardancy, toughness, antibacterial, dielectric and recycling properties, *Int. J. Biol. Macromol.* 278 (2024) 134933.
- [26] T. Chu, Y. Lu, B. Hou, P. Jafari, Z. Zhou, H. Peng, S. Huo, P. Song, The application of ammonium polyphosphate in unsaturated polyester resins: a mini review, *Polym. Degrad. Stab.* 225 (2024) 110796.
- [27] Y. Zhan, X. Wu, S. Wang, B. Yuan, Q. Fang, S. Shang, C. Cao, G. Chen, Synthesis of a bio-based flame retardant via a facile strategy and its synergistic effect with ammonium polyphosphate on the flame retardancy of polylactic acid, *Polym. Degrad. Stab.* 191 (2021) 109684.
- [28] L. Meng, X. Li, M. Liu, C. Li, L. Meng, S. Hou, Modified ammonium polyphosphate and its application in polypropylene resins, *Coatings* 12 (11) (2022) 1738.
- [29] Z.B. Shao, J. Zhang, R.K. Jian, C.C. Sun, X.L. Li, D.Y. Wang, A strategy to construct multifunctional ammonium polyphosphate for epoxy resin with simultaneously high fire safety and mechanical properties, *Compos. Part A Appl. Sci. Manuf.* 149 (2021) 106529.
- [30] Y. Zhang, L. Liu, M. Yao, J. Feng, Y. Xue, P.K. Annamalai, V. Chevali, T. Dinh, Z. Fang, H. Liu, Functionalizing lignin by in situ solid-phase grafting ammonium polyphosphate for enhancing thermal, flame-retardant, mechanical, and UV-resistant properties of polylactic acid, *Chem. Eng. J.* 495 (2024) 153429.
- [31] Y. Tan, Z.B. Shao, X.F. Chen, J.W. Long, L. Chen, Y.Z. Wang, Novel multifunctional organic–inorganic hybrid curing agent with high flame-retardant efficiency for epoxy resin, *ACS Appl. Mater. Interfaces* 7 (32) (2015) 17919–17928.
- [32] Y. Tan, Z.B. Shao, L.X. Yu, Y.J. Xu, W.H. Rao, L. Chen, Y.Z. Wang, Polyethyleneimine modified ammonium polyphosphate toward polyamine-hardener for epoxy resin: thermal stability, flame retardance and smoke suppression, *Polym. Degrad. Stab.* 131 (2016) 62–70.
- [33] G. Zeng, W. Zhang, X. Zhang, W. Zhang, J. Du, J. He, R. Yang, Study on flame retardancy of APP/PEPA/MoO₃ synergism in vinyl ester resins, *J. Appl. Polym. Sci.* 137 (35) (2020) 49026.
- [34] H. Du, J. Ren, X. Fu, W. Zhang, R. Yang, Simultaneous improvements of the fire safety, mechanical properties and water resistance of vinyl ester resin composites by introducing microencapsulated ammonium polyphosphate by polytriazole, *Compos. B. Eng.* 238 (2022) 109908.
- [35] Z.Z. Xu, J.Q. Huang, M.J. Chen, Y. Tan, Y.Z. Wang, Flame retardant mechanism of an efficient flame-retardant polymeric synergist with ammonium polyphosphate for polypropylene, *Polym. Degrad. Stab.* 98 (10) (2013) 2011–2020.
- [36] Z.B. Shao, C. Deng, Y. Tan, M.J. Chen, L. Chen, Y.Z. Wang, Flame retardation of polypropylene via a novel intumescent flame retardant: ethylenediamine-modified ammonium polyphosphate, *Polym. Degrad. Stab.* 106 (2014) 88–96.
- [37] Z.B. Shao, C. Deng, Y. Tan, L. Yu, M.-J. Chen, L. Chen, Y.Z. Wang, Ammonium polyphosphate chemically-modified with ethanolamine as an efficient intumescent flame retardant for polypropylene, *J. Mater. Chem. A* 2 (34) (2014) 13955–13965.
- [38] Z. Chen, M. Jiang, Z. Chen, T. Chen, Y. Yu, J. Jiang, Preparation and characterization of a microencapsulated flame retardant and its flame-retardant mechanism in unsaturated polyester resins, *Powder Technol.* 354 (2019) 71–81.
- [39] J. Xu, Y. Niu, Z. Xie, F. Liang, F. Guo, J. Wu, Synergistic flame retardant effect of carbon nanohorns and ammonium polyphosphate as a novel flame retardant system for cotton fabrics, *Chem. Eng. J.* 451 (2023) 138566.
- [40] N. Graf, E. Yegen, T. Gross, A. Lippitz, W. Weigel, S. Krakert, A. Terfort, W. E. Unger, XPS and NEXAFS studies of aliphatic and aromatic amine species on functionalized surfaces, *Surf. Sci.* 603 (18) (2009) 2849–2860.
- [41] J. Yan, P. Xu, P. Zhang, H. Fan, Surface-modified ammonium polyphosphate for flame-retardant and reinforced polyurethane composites, *Colloids Surf. A Physicochem. Eng. Asp.* 626 (2021) 127092.
- [42] T. Zhu, G. Guo, W. Li, M. Gao, Synergistic flame retardant effect between ionic liquid-functionalized imogolite nanotubes and ammonium polyphosphate in unsaturated polyester resin, *ACS Omega* 7 (51) (2022) 47601–47609.
- [43] Z. Li, T. Fu, D.M. Guo, J.H. Lu, J.H. He, L. Chen, W.D. Li, Y.Z. Wang, Trinity flame retardant with benzimidazole structure towards unsaturated polyester possessing high thermal stability, fire-safety and smoke suppression with in-depth insight into the smoke suppression mechanism, *Polym* 275 (2023) 125928.
- [44] L.P. Dong, C. Deng, R.M. Li, Z.J. Cao, L. Lin, L. Chen, Y.Z. Wang, Poly (piperaziny phosphamide): a novel highly-efficient charring agent for an EVA/APP intumescent flame retardant system, *RSC Adv.* 6 (36) (2016) 30436–30444.
- [45] E. Sanned, R.A. Mensah, M. Försth, O. Das, The curious case of the second/end peak in the heat release rate of wood: a cone calorimeter investigation, *Fire Mater.* 47 (4) (2023) 498–513.
- [46] M. Gao, J. Wang, Y. Gao, J. Chen, L. Qian, Z. Qiao, Ionic liquids modified MXene as a flame retardant synergist for the unsaturated polyester resin, *J. Vinyl Addit. Technol.* 30 (2) (2024) 530–542.
- [47] T. Sai, X. Ye, B. Wang, Z. Guo, J. Li, Z. Fang, S. Huo, Transparent, intrinsically fire-safe yet impact-resistant poly (carbonates-b-siloxanes) containing Schiff-base and naphthalene-sulfonate, *J. Mater. Sci. Technol.* 225 (2024) 11–20.
- [48] G. Ye, S. Huo, C. Wang, Q. Zhang, H. Wang, P. Song, Z. Liu, Strong yet tough catalyst free transesterification vitrimer with excellent fire retardancy, durability, and closed loop recyclability, *Small* 20 (45) (2024) 2404634.
- [49] C. Wang, S. Huo, G. Ye, Q. Zhang, C.F. Cao, M. Lynch, H. Wang, P. Song, Z. Liu, Strong self-healing close-loop recyclable vitrimers via complementary dynamic covalent/non-covalent bonding, *Chem. Eng. J.* 500 (2024) 157418.
- [50] G. Ye, S. Huo, C. Wang, Q. Zhang, B. Wang, Z. Guo, H. Wang, Z. Liu, Fabrication of flame-retardant, strong, and tough epoxy resins by solvent-free polymerization with bioderived, reactive flame retardant, *Sustain. Mater. Technol.* 39 (2024) e00853.
- [51] A. Sadezky, H. Muckenhuber, H. Grothe, R. Niessner, U. Pöschl, Raman microspectroscopy of soot and related carbonaceous materials: Spectral analysis and structural information, *Carbon* 43 (8) (2005) 1731–1742.
- [52] D. Zhao, J. Wang, X.L. Wang, Y.Z. Wang, Highly thermostable and durably flame-retardant unsaturated polyester modified by a novel polymeric flame retardant containing Schiff base and spirocyclic structures, *Chem. Eng. J.* 344 (2018) 419–430.
- [53] X.H. Shi, Q.Y. Liu, X.L. Li, A.K. Du, J.W. Niu, Y.M. Li, Z. Li, M. Wang, D.Y. Wang, Construction phosphorus/nitrogen-containing flame-retardant and hydrophobic coating toward cotton fabric via layer-by-layer assembly, *Polym. Degrad. Stab.* 197 (2022) 109839.

- [54] Y.M. Li, S.L. Hu, H.P. Fang, Y. Deng, C.D. Yang, D.Y. Wang, The designation of intrinsic flame-retarding vinyl ester resins with high mechanical property, optical transparency and degradability, *Chem. Eng. J.* 479 (2024) 147786.
- [55] J.P. Gallas, J.M. Goupil, A. Vimont, J.C. Lavalley, B. Gil, J.P. Gilson, O. Miserque, Quantification of water and silanol species on various silicas by coupling IR spectroscopy and in-situ thermogravimetry, *Langmuir* 25 (10) (2009) 5825–5834.
- [56] V. Realinho, L. Haurie, J. Formosa, J.I. Velasco, Flame retardancy effect of combined ammonium polyphosphate and aluminium diethyl phosphinate in acrylonitrile-butadiene-styrene, *Polym. Degrad. Stab.* 155 (2018) 208–219.